BOREAL ENVIRONMENT RESEARCH 14: 515–526
ISSN 1239-6095 (print) ISSN 1797-2469 (online)

Helsinki 31 August 2009

Physical and chemical characteristics of aerosol particles and cloud-droplet activation during the Second Pallas Cloud Experiment (Second PaCE)

Niku Kivekäs[1)], Veli-Matti Kerminen[1)], Tomi Raatikainen[1)], Petri Vaattovaara[2)], Ari Laaksonen[1)2)] and Heikki Lihavainen[1)]

[1)] *Finnish Meteorological Institute, P.O. Box 503, FI-00101 Helsinki, Finland*
[2)] *Department of Physics, University of Kuopio, P.O. Box 1627, FI-70211 Kuopio, Finland*

Received 16 Feb. 2009, accepted 6 May 2009 (Editor in charge of this article: Jaana Bäck)

Kivekäs, N., Kerminen, V.-M., Raatikainen, T., Vaattovaara, P., Laaksonen, A. & Lihavainen, H. 2009: Physical and chemical characteristics of aerosol particles and cloud-droplet activation during the Second Pallas Cloud Experiment (Second PaCE). *Boreal Env. Res.* 14: 515–526.

The Second Pallas Cloud Experiment (Second PaCE) was conducted at the Pallas-Sodankylä Global Atmosphere Watch (GAW) station in northern Finland from 16 September to 6 October 2005. Measured parameters included aerosol number size distribution, aerosol chemical composition, aerosol hygroscopic growth factor, cloud droplet number size distribution and meteorological parameters. Air mass back trajectories were also calculated. The particulate volume and the inorganic fraction (IO) of particulate mass depended strongly on the air-mass history: central European air masses contain much more particulate matter and have higher IO than marine air masses. The hygroscopic growth factor of particles was positively correlated with the IO. Aerosol activation into cloud droplets was studied for accumulation mode particles (d_p > 100 nm). The activation of these particles did not show clear dependency on the number concentration of accumulation mode particles or on IO. These two parameters were positively correlated and their effects on the particle activation could not be separated.

Introduction

In global climate modeling, aerosols and their interaction with clouds and the climate system constitute the largest uncertainty in radiative forcing (IPCC 2007). The formation, lifetime and radiative properties of clouds depend in a complicated manner on atmospheric aerosols, including their loading, size distribution and chemical composition (e.g. Koren *et al*. 2007, Baker and Peter 2008, Rosenfeld *et al*. 2008). Detailed information on aerosol–cloud interaction is therefore needed to improve our ability to describe and predict the behavior of the current and future climate system.

The most comprehensive investigations related to aerosol–cloud interactions are various kinds of cloud condensation nuclei (CCN) closure studies (e.g. Snider *et al*. 2003, Gasparini *et al*. 2006, Medina *et al*. 2007). Much fewer experimental data is available on influence of aerosols on cloud microphysics (e.g. Henning *et al*. 2002, Koch *et al*. 2003, Mertes *et al*. 2005, Wang *et al*. 2007, Lihavainen *et al*. 2008), and in only a very few studies aerosol and cloud properties have been measured at the same time and place.

The Pallas-Sodankylä Global Atmospheric Watch (GAW) station, located in a remote continental site in northern Finland, provides a suitable site to investigate aerosol–cloud interactions via ground-based measurements (Kerminen *et al*. 2005, Komppula *et al*. 2005, Lihavainen *et al*. 2007, 2008). Here, we complement our earlier Pallas cloud studies by presenting and analyzing data from an intensive field campaign with simultaneous measurements of cloud microphysics and aerosol physical, chemical and hygroscopic properties. Our main objective is to get further insight into how cloud microphysical properties, especially cloud droplet number concentration, depend on aerosol physico-chemical properties at our measurements site, and whether significant differences in aerosol–cloud relations can be observed between different air mass types in the northern Scandinavian boreal and subarctic regions.

Material and methods

Measurement site and conditions

The Second Pallas Cloud Experiment (Second PaCE), an intensive three-week campaign for measuring aerosol and cloud properties, was conducted by the Finnish Meteorological Institute and by the University of Kuopio at the Pallas-Sodankylä GAW station (Hatakka *et al*. 2003).

The station consists of several measurement sites, of which only the main site Sammaltunturi (67°58´N, 24°07´E, 560 m a.s.l., in Muonio, Lapland) is considered here. This site is located slightly above the tree line on a top of a fell (Arctic round-topped hill), which rises about 300 m above the surrounding area. The area is mainly lowland covered with boreal forest and swamps to the east and west of the station, but there are higher fells north and south of the station. The station is located inside the Pallas-Yllästunturi national park. The area outside the park the area is very sparsely populated. The closest municipalities are Muonio with some 2500 inhabitants about 20 km south-west from the station and Kittilä, with about 6000 inhabitants, 40 km south-east from the station. The station is suitable for studies on aerosol–cloud interaction measurements (Kerminen *et al*. 2005, Komppula *et al*. 2005, Lihavainen *et al*. 2007, 2008), since the station is inside cloud for a substantial fraction of time. As the station is only 300 m above the surrounding area, only low clouds can be studied.

The measurements were conducted from 16 September to 6 October 2005. This time of the year was chosen to maximize the chances of the station being inside a cloud. During the first third of the measurement period, the air masses were mostly coming from the North Atlantic or the Arctic Ocean. The rest of the measurement period was characterized by air masses coming from south or south-west over central Europe or the British Islands and Scandinavia. The ambient temperature at 570-m altitude a.s.l. varied from –4.2 °C to +11.3 °C during the measurement period, and average and standard deviation of temperature were +4.7 °C and 3.0 °C, respectively. The temperature was below 0 °C for 10% of the time. The average (± SD) ambient pressure and wind speed were 940 ± 8 hPa and 7.4 ± 2.7 m s^{-1}, respectively. During the measurement campaign the station was inside cloud (visibility below 200 m) for 25% of the time, but only 12% of the time was there any rain. Low clouds typically appeared during nights and disappeared around noon.

Instrumentation

The instruments used to measure the particle and cloud droplet properties are listed in Table 1.

Differential mobility particle sizer (DMPS)

Two differential mobility particle sizers (DMPS) were used to measure the aerosol number size distribution. Both DMPSs had the structure described by Komppula *et al*. (2005). One DMPS ($DMPS_{tot}$) was attached to a so-called total air inlet, which lets in all particles including cloud droplets (but not rain drops). The cloud droplets were then evaporated, and the dry cloud-condensing nuclei (CCN) were measured among the non-activated particles. The other

DMPS ($DMPS_{PM2.5}$) was attached to a PM2.5 inlet, which prevented the cloud droplets, and therefore CCN from entering the system. Thus, when a cloud was present $DMPS_{PM2.5}$ measured only those particles that were not activated. Each of the DMPSs measured the dry diameter range 7–500 nm in 30 discrete size fractions. The whole size range was scanned in five minutes by each DMPS, after which the data was saved.

Komppula *et al*. (2005) showed that the cloud droplet number concentration and D_{50} activation diameter (diameter at which 50% of particles activate) can be calculated from the data produced by two DMPSs, one being inside the cloud and the other being outside the cloud. Komppula *et al*. (2005) used two DMPSs at two different measurement sites placed at 6-km horizontal and 220-m vertical distance from each other. This distance made their result vulnerable to speculation whether the two sites represented the same air mass. To avoid the possible errors coming from the distance between the instruments, in our study the instruments were located at the same site.

Forward scattering scanning probe (FSSP)

The cloud droplet number size distributions (3–47 μm) were measured with a FSSP-100 Forward Scattering Spectrometer Probe (Particle Measuring Systems Inc., USA) with upgraded electronics (Droplet Measurement Technologies, Boulder, Colorado, USA) (Brenguier 1989). The FSSP was placed onto a rotating platform with the inlet always facing into the wind. Since droplet concentrations during the operation period of FSSP relatively low (< 300 cm^{-3}), the FSSP data were not corrected for coincidence or dead-time losses (Baumgardner *et al*. 1985). The FSSP was calibrated after the campaign. The cloud droplet number and size distribution were the only cloud microphysical properties used in this study.

Aerosol mass spectrometer (AMS)

The chemical composition and mass concentration of particulate matter were measured with an Aerodyne quadrupole aerosol mass spectrometer

Table 1. The instrumentation and data parameters used for measuring the aerosol and cloud droplet properties during the measurement campaign. The total air inlets allow all particles to pass through, whereas the PM2.5 inlet lets through only particles with $d_p < 2.5$ μm.

Instrument	Measured parameter	Air inlet	Measured diameter range	Period
$DMPS_{tot}$ (all particles)	Number size distribution	Total	7–500 nm (dry diameter)	16 Sep.–6 Oct.
$DMPS_{PM2.5}$ (interstitial particles)	Number size distribution	PM2.5	7–500 nm (dry diameter)	16 Sep.–6 Oct.
FSSP	Cloud droplet number size distribution	Own inlet (Total)	3–47 μm (wet diameter)	30 Sep.–5 Oct.
AMS	Mass concentration	Total	60–600 nm	21 Sep.–6 Oct.
HTDMA	Hygroscopic growth	Total	30–150 nm	19 Sep.–4 Oct.

(AMS) (Jayne *et al*. 2000, Allan *et al*. 2003, Canagaratna *et al*. 2007). Inorganic species ammonium (NH_4^+), sulfate (SO_4^{-2}) and nitrate (NO_3^-) were measured, as well as the organic matter. The instrument is not capable of measuring sea salt, black carbon or crustal material because they do not evaporate at the temperature of 600 °C used to vaporize the particles in the instrument. The measured concentrations of non-sea-salt chloride (nss-Cl^-) and polycyclic aromatic hydrocarbons (PAH) were within the noise, and were not included in the analysis.

Rural and background aerosols contain mainly oxidized organic aerosol (OOA) species (Zhang *et al*. 2007). According to Lanz *et al*. (2007), there are two OOA types so that type 1 (OOA-1) is processed, aged and highly oxidized and type 2 (OOA-2) is less processed and oxidized OOA fraction. When organic matter is composed of OOA-1 and OOA-2, peaks caused by organic matter at $m/z = 44$ and $m/z = 43$ originate mostly from OOA-1 and OOA-2 species, respectively. These peaks are also present in the mass spectra of aerosols from wood burning and fresh traffic emissions (Lanz *et al*. 2007), but no indication of that type of emissions were found. Therefore, ratio of the peaks at $m/z = 44$ and $m/z = 43$ is indicative of OOA-1 and OOA-2 concentration ratio and thereby organic aerosol oxidation state and age.

The transmission efficiency of the AMS is practically 100% in the size range 60–600 nm. Particles smaller than 60 nm in diameter have usually only a minor contribution to the mass concentration of any species. Although the AMS can measure some particles with diameters up to 1500 nm (Drewnick *et al*. 2009), because the transmission efficiency of the AMS is low for such large particles, the AMS measures approximately the PM1 size fraction. Particle volume–size distributions were calculated from the DMPS data, and most particulate volume always was in particles with diameter below 350 nm. No indication of another particle mode with higher diameter was found. Based on this, we can assume that the AMS measures approximately the same particle size range that the DMPSs described above measure.

The mass concentrations measured with the AMS depend largely on the mass calibration of the instrument. The calibration was not performed at the measurement site, even though it would have been the normal procedure. The concentrations of all species are multiplied by the same calibration value, so an incorrect calibration value has the same relative effect on all mass concentrations, but does not affect the mass fractions of each species.

Hygroscopicity Tandem Differential Mobility Analyzer (H-TDMA)

Hygroscopic properties of the dried aerosol population were measured with a Hygroscopicity-Tandem Differential Mobility Analyzer (H-TDMA) (Joutsensaari *et al*. 2001). In this instrument, the dried aerosol flow goes first through one DMA-unit. Next, the selected size fraction is led to humidifier, a chamber with controlled relative humidity. From the humidifier the moist aerosol is the led to another DMA-unit without drying, and is classified according to its wet diameter. The controlled growth of a narrow size fraction allows the calculation of growth factors for particles having different dry diameters.

In our measurements, the humidifier was kept at about 90% relative humidity, and the measured dry diameters were 30, 50, 80, 100 and 150 nm. The relative humidity of the aerosol flow in the second DMA was kept about 2%–3% lower than that of the sheath flow.

Other measurements

Other than aerosol parameters, meteorological conditions were also measured at the site. The measured meteorological parameters were the temperature, dew point, relative humidity, air pressure, visibility, wind speed, wind direction, global solar radiation and rain intensity and type. The wind parameters were measured at 6 m above ground, temperature and relative humidity at 4 m above ground and pressure at 2 m above ground. (Hatakka *et al*. 2003) The presence of clouds was estimated from measured visibility, from relative humidity, and verified from photographs of the site taken automatically every 30 minutes during the day.

The air mass history was evaluated by calculating the five-day back trajectories using the HYSPLIT (HYbrid Single-Particle Lagrangian Integrated Trajectory) model (http://www.arl.noaa.gov/ready/hysplit4.html), which calculates the trajectory of a single pollutant particle without any dispersion. The data were manually classified according to the air mass history into three categories: continentally-influenced European, marine and "mixed" air masses that have spent considerable amount of time both over sea and land. In order to be classified as marine, the air mass had to originate from the North Atlantic or the Arctic Ocean, and could not have passed over central Europe, the British Islands or southern Scandinavia. The European air masses had to originate from central or eastern Europe, and had to spend less than 10 hours after leaving these regions before entering Pallas. All other air masses were classified as mixed cases.

Data processing

All data were converted into 1-h averages. If there were data from less than 30 minutes of any given hour, that data were excluded from the averaging, except for the data form the HTDMA, which measures about 10 minutes for each size class. The different aerosol data sets were also checked for contamination caused by people entering the site with vehicles. Such periods produced sharp peaks that were removed from the data. The six smallest size fraction (diameter 7–15 nm) of the DMPS data were not included in the total particle number calculations or in the cloud activation calculations, because the counting efficiencies of the DMPSs differed from each other in that size range.

Results

General characteristics of the aerosol population

The 1-h average particle number concentration (measured with $DMPS_{tot}$) varied in the range 56–3900 cm^{-3} with a median of 710 cm^{-3} and average of 920 cm^{-3}. The number concentration time series consisted of a base level below 500 cm^{-3} and frequent peaks reaching above 1000 cm^{-3}. Such peaks could be seen in all air mass types, but the low number concentration periods were typically associated with marine air. The number concentration of accumulation mode (N_{Acc}, particle diameter $d_p > 100$ nm) particles had a good correlation with the air mass type as well, being clearly lowest in marine air and highest in European air masses. In European air masses the number concentration of accumulation mode particles was on average even higher than that of Aitken mode (N_{Ait}, 20 nm < d_p < 100 nm) (Table 2).

The particle volume concentration was also calculated from the $DMPS_{tot}$ data by assuming that all particles were spherical. These data were then compared with the PM1 aerosol mass concentration data measured with the AMS (Fig. 1), and a good correlation ($R = 0.99$, $p < 0.001$) was found. The median ratio of mass to volume was 1.07 g cm^{-3}, and 82% of the mass to volume ratios were in the range from 0.5 g cm^{-3} to 1.5 g cm^{-3}. The mass concentration measured with the AMS showed the same peaks and low concentration periods as the volume concentration calculated from the $DMPS_{tot}$ results. During the concentration peaks the AMS showed slightly lower values than the DMPS. This might be explained by a higher fraction of non-volatile materials, such as black carbon, in particles during high mass concentration periods, but no data on non-volatile material were available in this study. During the low concentration periods the AMS values were about the same or slightly higher than those from the DMPS.

The measured mass-to-volume ratio (density) was lower than that observed in some other studies (McMurry *et al*. 2002, Saarikoski *et al*. 2005, Kannosto *et al*. 2008). However, there were several factors influencing our measurements. The AMS is unable to measure sea salt, black carbon or dust, which are measured by the DMPS and therefore included in the volume calculations, lowering the mass to volume ratio. However, the main reason for the low mass-to-volume ratio is probably the uncertainties related to the mass calibration of the AMS.

The total PM1 mass concentration (m_{tot}) of particulate matter differed between the different

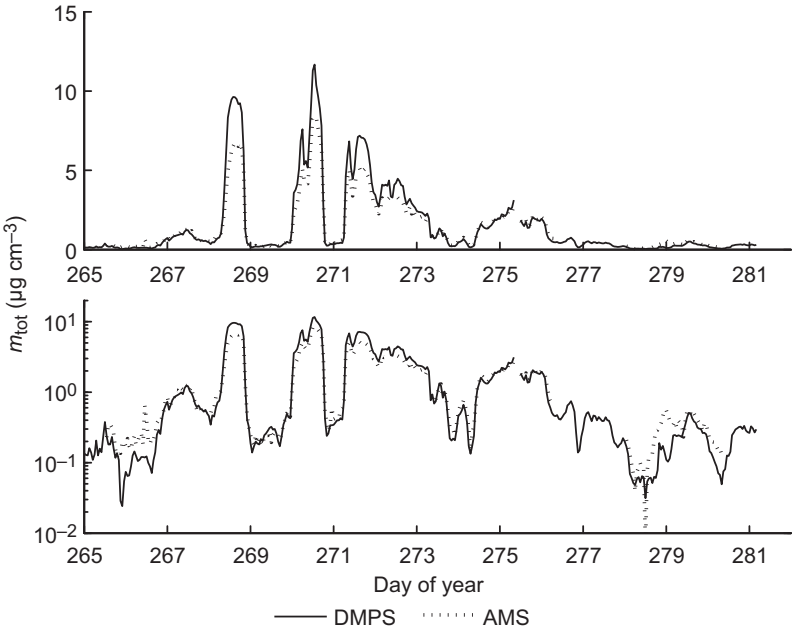

Fig. 1. The mass concentration of all measured particles (m_{tot}) measured with AMS and with $DMPS_{tot}$, assuming spherical particles and constant density of 1 g cm^{-3}.

air masses. In marine air masses the m_{tot} was very low, being below 1.0 μg m^{-3} for 96% of the time. The mean value of m_{tot} in marine air masses was 0.35 μg m^{-3}. These concentrations are close to the AMS detection limit of about 0.1 μg m^{-3}. In European air masses, m_{tot} reached values as high 8.29 μg m^{-3}, and was less than 1.0 μg m^{-3} for only 10% of the time. The mean value of m_{tot} in European air masses was 4.62 μg m^{-3}. As expected, the mixed air masses fell between these two extremes, having a mean m_{tot} of 1.51 μg m^{-3}.

The inorganic fraction (IO) of m_{tot} followed the air mass type as well. In marine air masses, the mean IO was 23%, whereas it was 37% in mixed and 44% in European air masses. The inorganic fraction consisted of 12% NO_3^-, 64% SO_4^{2-} and 25% NH_4^+ (median values). The relative contribution of different inorganic species did not depend on air mass type. In marine air masses some of the mass concentrations were below the detection limits of the instrument (Drewnick *et al*. 2009) so the relative contributions could not be calculated reliably.

The particle hygroscopic growth factors (GF) at 90% relative humidity were measured for particles having dry diameters of 30, 50, 80, 100

Table 2. The number concentrations of accumulation mode particles (N_{Acc}), Aitken mode particles (N_{Ait}) and total particle population (7 nm < d_p < 500 nm, N_{tot}), as well as the total volume concentration (V_{tot}) calculated from the DMPS data and the total mass concentration (m_{tot}) from the AMS data during the Second PaCE measurement campaign.

Air mass	Value	N_{Acc} (cm^{-3})	N_{Ait} (cm^{-3})	N_{tot} (cm^{-3})	V_{tot} (μm^3 cm^{-3})	m_{tot} (μg m^{-3})
Marine	Mean	70	779	1041	0.29	0.35
	Median	55	366	535	0.24	0.26
Mixed	Mean	322	733	1090	1.61	1.58
	Median	278	549	1063	1.12	1.50
European	Mean	965	561	1531	6.13	4.62
	Median	1015	502	1576	6.53	5.00
Total	Mean	221	573	916	1.19	1.51
	Median	73	421	712	0.31	0.64

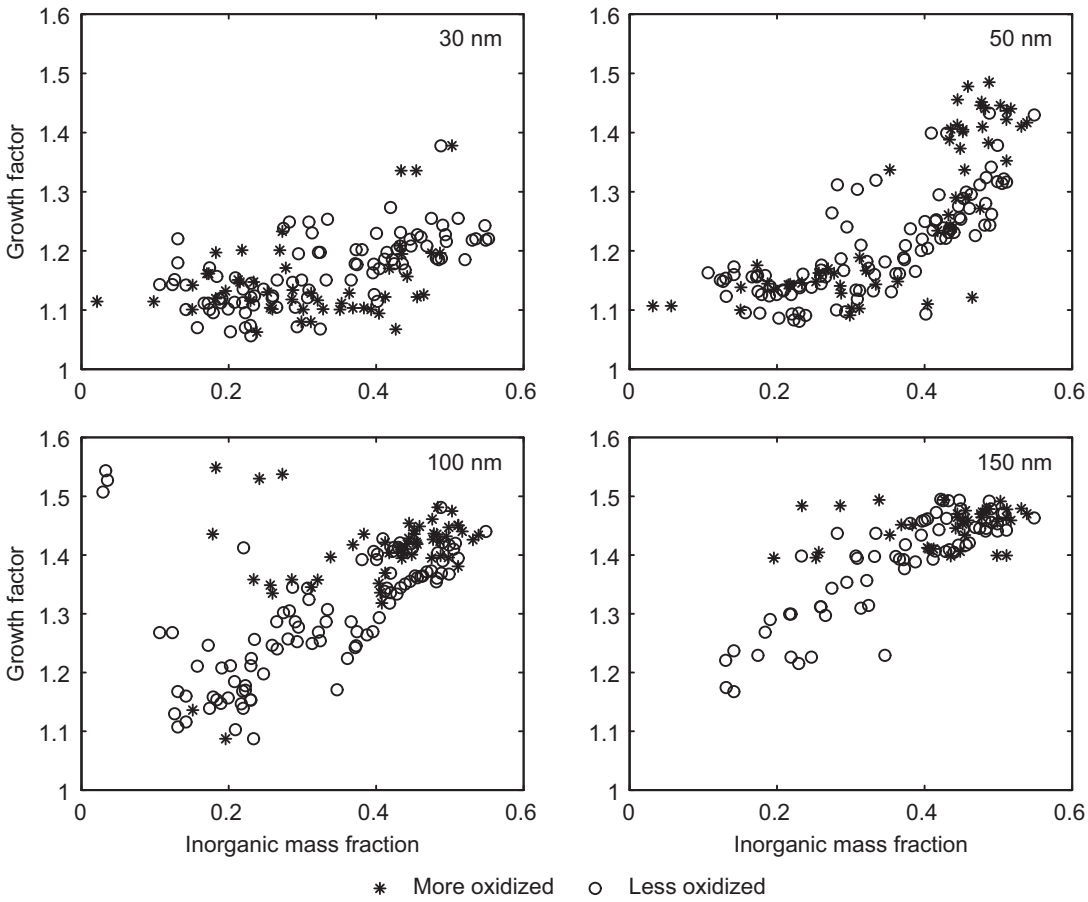

Fig. 2. Growth factors in 90% relative humidity for dry diameter classes 30 nm (upper left), 50 nm (upper right), 100 nm (lower left) and 150 nm (lower right) as a function of inorganic fraction of the total particulate mass. The more oxidized (the ratio between the peaks at m/z = 44 and m/z = 43 was larger than 1.75), and the less ozidized (the ratio between the peaks at m/z = 44 and m/z = 43 was smaller than or equal to 1.75) aerosol populations are shown.

and 150 nm. The growth factors varied from about 1.1 to 1.5 for all the particle sizes. The average growth factor increased systematically with an increasing dry particle diameter (Table 3). The size dependency of GF can be at least partially explained by the increased Kelvin effect in small particles.

In all size classes, the value of GF increased with an increasing inorganic fraction of the particle mass. In the two largest size classes (d_p = 100 nm and d_p = 150 nm) the growth factor depended also on the oxidation state of the organic species in the particles: when organic species were highly oxidized, the growth factor was high, even when the inorganic fraction was low. In the smaller size classes the effect of the oxidation state was not as clear (Fig. 2).

Table 3. The average growth factors (GF) and the corresponding 25% and 75% values during the measurement campaign for particles in five different size classes.

Dry diameter (nm)	Average GF	Lower 25%	Upper 25%
30	1.16	1.11	1.20
50	1.22	1.14	1.28
80	1.26	1.16	1.37
100	1.32	1.22	1.41
150	1.44	1.36	1.46

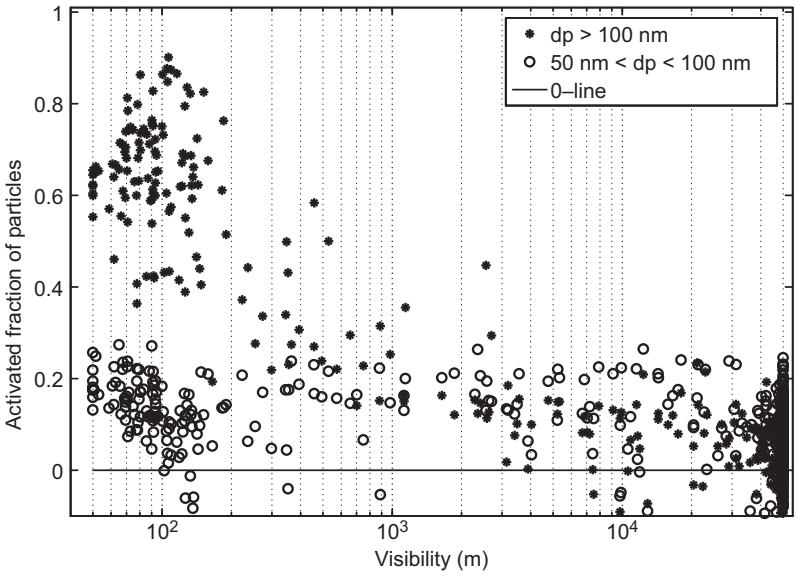

Fig. 3. Activated fraction of accumulation mode (d_p > 100 nm) particles and the smaller (50 nm < d_p < 100 nm) particles calculated from the DMPS results as function of visibility.

Relations between aerosol and cloud droplet properties

Uncertainties related to determining cloud droplet number concentration

The number concentration of activated particles was calculated from the difference between the two DMPSs. This concentration difference can be assumed to equal the cloud droplet number concentration (CDNC) in freshly formed clouds (Komppula *et al*. 2005). The CDNC was also measured directly with the FSSP. The FSSP was operational only for a little more than two days, so relatively few FSSP data were available for comparison. From the DMPS and FSSP data, the ratio of the CDNC measured with the FSSP to that calculated from the DMPS data had a median value of 1.05, being in the range of 0.75–1.25 for 63% of the time.

The method of getting the activated particles by subtracting one DMPS size distribution from the other is sensitive to errors in either one of the size distributions. This method also does not distinguish between activated particles and particles scavenged by cloud droplets. These errors can lead to uncertain and even non-physical values of different activation parameters. In order to study the effect of these uncertainties, the fraction of accumulation mode (particle diameter d_p > 100 nm) particles that was activated into cloud droplets (Act_{100}) and the corresponding fraction of smaller (50 nm < d_p < 100 nm) particles (Act_{50}) were plotted against visibility at the measurement site (Fig. 3). The particles with diameters smaller than 50 nm were not taken into account in the activation calculations, because differences in the size distribution at this size range are caused mainly by processes other than cloud droplet activation (Komppula *et al*. 2005).

As expected, Act_{100} decreased with increasing visibility. The highest values of Act_{100} (up to 90%) were measured during periods when visibility was below 200 m. At higher visibilities Act_{100} decreased towards zero. There was variability in Act_{100} resulting from the uncertainties in the method for calculating Act_{100}, as mentioned above. Even when the visibility was 50 km (maximum) the calculated Act_{100} varied from –15% to +20%.

The value of Act_{50} varied from –10% to +20% almost independent of visibility. This means that the activation of sub-100 nm particle, if occurring, was buried under measurement uncertainties in this data set. As a result, no further analysis on Act_{50} was made in this paper.

Particle activation into cloud droplets

The 1-h average data were divided into three categories according to visibility at the measure-

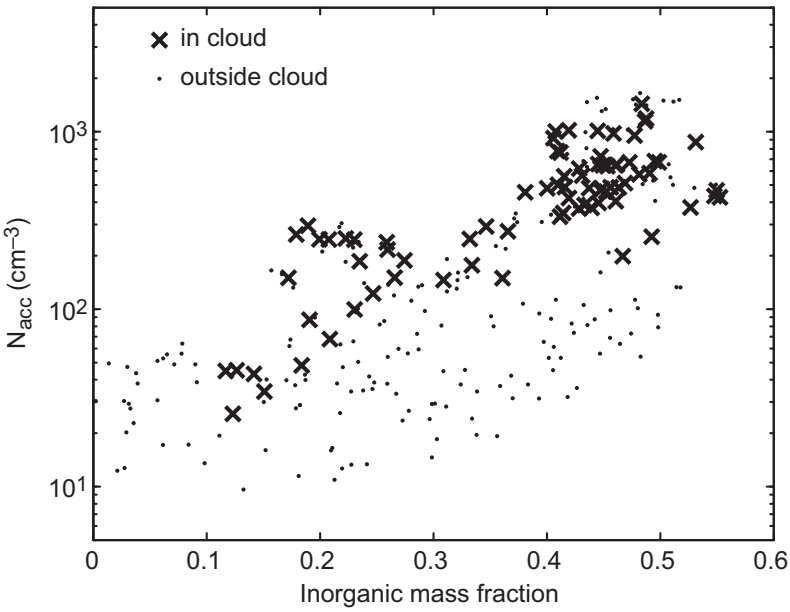

Fig. 4. The number concentration of accumulation mode (d_p > 100 nm) particles measured with $DMPS_{tot}$ as function of inorganic fraction of particle mass (PM1) for both in-cloud and outside cloud cases.

ment site. These categories had visibilities < 200 m (cloud, 23% of time), 200–3000 m (indeterminate, 7% of time) and > 3000 m (no cloud, 70% of time). The first two categories did not differ much from each other in number concentrations of Aitken or accumulation mode particles, in inorganic fraction of particle mass, or in air mass type (Table 4). The third category (no cloud) had typically much lower particle concentrations in the accumulation mode and also lower inorganic fraction than the two other categories. The "no cloud" cases were also typically associated with marine air masses, whereas the other two types (cloud and unclear) were more often associated with mixed or European air masses.

The number concentration of accumulation mode particles (N_{acc}) was positively correlated (R = 0.61) with the inorganic fraction of particle mass (IO). This dependency made it difficult to separate the effects of these two factors on cloud droplet activation. There were no cases in which IO was low and simultaneously N_{acc} was high (Fig. 4). For any given value range of IO, cloudy cases were restricted to the highest values of N_{acc}. When IO was high and N_{acc} was low, no clouds were present.

When clouds were present, the average activated fraction of accumulation mode particles (Act_{100}) was 66%, and 10- and 90-percentiles of the activated fraction were 43% and 82%, respectively. There was a weak dependency between Act_{100} and N_{acc}, with Act_{100} decreasing slightly with increasing values of N_{acc}. Act_{100} did not show any systematic dependency on the soluble fraction of particle mass.

The finding that smaller Act_{100} at was associated higher particle number concentration can be explained by the amount of water vapor available for condensation. With a high number concentration of particles, the maximum super-

Table 4. The visibility criteria for the three categories, and median values of accumulation mode (N_{acc}) and Aitken mode (N_{Ait}) number concentration, activated fraction of accumulation mode particles (Act_{100}) and inorganic fraction of particle mass (IO).

Category	Visibility (m)	N_{acc} (cm^{-3})	N_{Ait} (cm^{-3})	Act_{100} (%)	IO (%)
Cloud	0–200	293	500	65	42
Indeterminate	200–3000	503	536	26	45
No cloud	> 3000	54	372	4	30

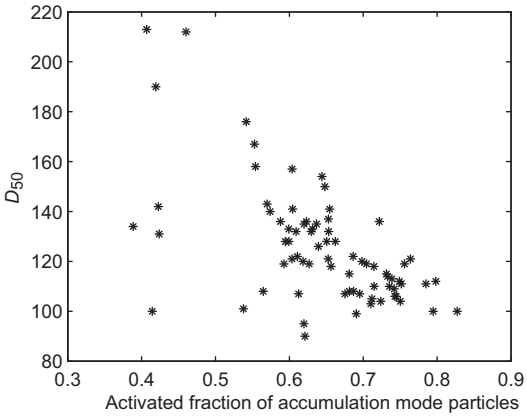

Fig. 5. The diameter in which 50% of particles with that diameter activate (D_{50}) as function of the activated fraction of accumulation mode (d_p > 100 nm) particles measured with $DMPS_{tot}$.

saturation reached by the air parcel is decreased, making the smaller and less hygroscopic particles less likely to be activated (e.g. Nenes *et al*. 2001, Chuang 2006). Particles with a high inorganic mass fraction (soluble particles) should be activated at low supersaturations according to Köhler theory (Köhler 1936). In our data set, however, a high inorganic fraction was associated with a high number concentration of accumulation mode particles, having the opposite effects on the activation probability. It looks like the particle loading had a larger influence of cloud droplet activation than the chemical composition of particles during our measurements. The solubility of the organic fraction of m_{tot} also affects the activation in the same way as the inorganic fraction of particle mass, and this weakens the dependency between Act_{100} and IO.

The diameter at which 50% of particles with that diameter activate (D_{50}) is a parameter suitable for simplified cloud activation parameterizations (e.g. Kivekäs *et al*. 2008), as it roughly separates the activating particles from those that do not activate. When D_{50} is above 100 nm, it should behave roughly inversely to Act_{100}, assuming that the particle hygroscopicity is not size-dependent in that size range. In this study D_{50} did not show any clear relation to the number concentration of accumulation mode particles, or to the inorganic fraction of particle mass. As expected, however, there was a clear inverse relation between D_{50} and Act_{100} (Fig. 5). When the activated fraction was high, D_{50} was low and *vice versa*.

Summary and conclusions

Aerosol and cloud parameters were measured at Pallas-Sodankylä GAW station from 16 September to 6 October 2005 as part of the Second Pallas Cloud Experiment (Second PaCE). The 1-h average particle number concentration ranged from 56 to 3900 cm^{-3} with a median of 710 cm^{-3} and average of 920 cm^{-3}. The average PM1 mass concentrations (m_{tot}) measured with an AMS depended strongly on air mass type, varying from 0.35 $\mu g\ m^{-3}$ in marine air to 4.62 $\mu g\ m^{-3}$ in European air masses. European air masses had also higher mass fractions of inorganic matter. Hygroscopic growth factor of particles increased with increasing inorganic fraction of particle mass and with increasing particle size. A higher oxidation state of the organic matter also increased the particle hygroscopicity.

The number concentration of activated particles was calculated from the difference between the distributions measured with two DMPSs similar to Komppula *et al*. (2005). The average fraction of accumulation mode particles that activated (Act_{100}) was 66 % when clouds were present. The activated fraction of smaller (50 nm < d_p < 100 nm) particles was clearly lower and less than the random error caused by the method of calculating the number of activated particles. Act_{100} was slightly smaller when the accumulation mode number concentration was high and the particles had to compete for the available water. In such cases the inorganic mass fraction was also high, but apparently not enough to cancel the effect of the large particle number concentration. The solubility of the organic mass fraction might also have been different in these cases. These effects led to no apparent relation between the activated fraction and the inorganic mass fraction. The D_{50} activation diameter did not show any systematic dependency on the number concentration of accumulation mode particles nor on the inorganic fraction of the particle mass. However, the value of D_{50} was dependent on Act_{100}, being smaller when Act_{100} was higher.

In this study, the observed particle number size distribution, chemical composition of particles and particle hygroscopic properties were related to each other, as they were all dependent on the air mass origin. The number of activated particles was determined by all these three properties combined, and distinguishing the contribution of any individual property was not possible. The vast majority of studies on aerosol–cloud interactions have, however, relied on either chemical or physical aerosol measurements, not both together. This can lead to erroneous conclusions on the aerosol–cloud interactions in a system where the physical, chemical and hygroscopic properties of aerosols are related to each other.

Acknowledgements: This work was funded by the Tor and Maj Nessling foundation and the Academy of Finland as part of the Finnish Centre of Excellence program (project nos. 211483, 211484 and 1118615). The authors would also like to thank all the people involved in the Second PaCE measurements campaign.

References

Allan J., Jimenez J., Williams P., Alfarra M., Bower K., Jayne J., Coe H. & Worsnop D. 2003. Quantitative sampling using an Aerodyne aerosol mass spectrometer 1. Techniques of data interpretation and error analysis. *J. Geophys. Res.* 108, 4090, doi:10.1029/2002JD002358.

Baker M.B. & Peter T. 2008. Small-scale cloud processes and climate. *Nature* 451: 299–300.

Baumgardner D., Strapp W. & Dye J.E. 1985. Evaluation of the forward scattering spectrometer probe, Part II. Correction for coincidence and dead-time losses. *J. Atmos. Oceanic Technol.* 2: 626–632.

Brenguier J. 1989. Coincidence and dead-time corrections for particle counters. Part ii: High concentration measurements with an FSSP. *J. Atmos. Oceanic Technol.* 6: 585–598.

Canagaratna M., Jayne J., Jimenez J., Allan J., Alfarra M., Zhang Q., Onasch T., Drewnick F., Coe H., Middlebrook A., Delia A., Williams L., Trimborn A., Northway M., DeCarlo P., Kolb C., Davidovits P. & Worsnop D. 2007. Chemical and microphysical characterization of ambient aerosols with the Aerodyne Aerosol Mass Spectrometer. *Mass Spec. Rev.* 26: 185–222.

Chuang P.Y. 2006. Sensitivity of cloud condensation nuclei activation processes to kinetic parameters. *J. Geophys. Res.* 111, D09201, doi: 10.1029/2005JD006529.

Drewnick F., Hings S.S., Alfarra M.R., Prevot A.S.H. & Borrmann S. 2009. Aerosol quantification with the Aerodyne Aerosol Mass Spectrometer: detection limits and ionizer background effects. *Atmos. Meas. Tech.* 2: 33–46.

Gasparini R., Collins D.R., Andrews E., Sheridan P.J., Ogren J.A. & Hudson J.G. 2006. Coupling aerosol size distributions and size-resolved hygroscopicity to predict humidity-dependent optical properties and cloud condensation nuclei spectra. *J. Geophys. Res.* 111, D05S13, doi:10.1029/2005JD006092.

Hatakka J., Aalto T., Aaltonen V., Aurela M., Hakola H., Komppula M., Laurila T., Lihavainen H., Paatero J., Salminen K. & Viisanen Y. 2003. Overview of the atmospheric research activities and results at Pallas GAW station. *Boreal Env. Res.* 8: 365–384.

Henning S., Weingartner E., Schmidt S., Wendisch M., Gäggeler H.W. & Baltensperger U. 2002. Size-dependent aerosol activation at the high-alpine site Jungfraujoch (3580 m a.s.l.). *Tellus* 54B: 82–95.

IPCC 2007. Summary for policymakers. In: *Climate change 2007: The physical science basis*, Contribution of Working Group I to the Fourth Assessment Report of the Intergovernmental Panel on Climate Change, Cambridge University Press, Cambridge, United Kingdom and New York, NY, p. 18.

Joutsensaari J., Vaattovaara P., Vesterinen M., Hämeri K. & Laaksonen A. 2001. A novel tandem differential mobility analyzer with organic vapor treatment of aerosol particles. *Atmos. Chem. Phys.* 1: 51–60.

Kannosto J., Virtanen A., Lemmetty M., Mäkelä J. M., Keskinen J., Junninen H., Hussein T., Aalto P. & Kulmala M. 2008. Mode resolved density of atmospheric aerosol particles. *Atmos. Chem. Phys.* 8: 5327–5337.

Kerminen V.-M., Lihavainen H., Komppula M., Viisanen Y. & Kulmala M. 2005. Direct observational evidence linking atmospheric aerosol formation and cloud droplet activation. *Geophys. Res. Lett.* 32, L14803, doi:10.1029/2005GL023130.

Kivekäs N., Kerminen V.-M., Anttila T., Korhonen H., Lihavainen H., Komppula M. & Kulmala M. 2008. Parameterization of cloud droplet activation using a simplified treatment of the aerosol number size distribution. *J. Geophys. Res.* 113, D15207, doi:10.1029/2007JD009485.

Koch D., Park J. & Del Genio A. 2003. Clouds and sulfate are anticorrelated: A new diagnostic for global sulfur models. *J. Geophys. Res.* 108(D24), 4781, doi:10.1029/2003JD003621.

Komppula M., Lihavainen H. & Kerminen V.-M. 2005. Measurements of cloud droplet activation of aerosol particles at a clean subarctic background. *J. Geophys. Res.* 110(D0), 6204, doi:10.1029/2004JD005200.

Koren I., Remer L.A., Kaufman Y.J., Rudich Y. & Martins J.V. 2007. On the twilight zone between clouds and aerosols. *Geophys. Res. Lett.* 34, L08805, doi:10.1029/2007GL029253.

Köhler H. 1936. The nucleus in and the growth of hygroscopic droplets. *Transactions of the Faraday Society* 43: 1152.

Lanz V.A., Alfarra M.R., Baltensperger U., Buchmann B., Hueglin C. & Prévôt A.S.H. 2007. Source apportionment of submicron organic aerosols at an urban site by factor analytical modelling of aerosol mass spectra. *Atmos. Chem. Phys.* 7: 1503–1522.

Lihavainen H., Komppula M., Kerminen V.-M., Järvinen H.,

Viisanen Y., Lehtinen K., Vana M. & Kulmala M. 2007. Size distributions of atmospheric ions inside clouds and in cloud-free air at a remote continental site. *Boreal Env. Res*. 12: 337–344.

Lihavainen H., Kerminen V.-M., Komppula M., Hyvärinen A.-P., Laakia J., Saarikoski S., Makkonen U., Kivekäs N., Hillamo R., Kulmala M. & Viisanen Y. 2008. Measurements of the relation between aerosol properties and microphysics and chemistry of low level liquid water clouds in northern Finland. *Atmos. Chem. Phys*. 8: 6925–6938.

Medina J., Nenes A., Sotiropoulou R.-E.P. Cotrell L.D., Ziemba L.D., Beckman P.J. & Griffin R.J. 2007. Cloud condensation nuclei closure during the International Consortium for Atmospheric Research on Transport and Transformation 2004 campaign: effects of size-resolved composition. *J. Geophys. Res*. 112, D10S31, doi:10.1029/2006JD007588.

McMurry P., Wang X., Park K. & Ehara K. 2002. The relationship between mass and mobility for atmospheric particles: a new technique for measuring particle density. *Aerosol Sci. Tech*. 36: 227–238.

Mertes S., Lehmann K., Nowak A., Massling A. & Wiedensohler A. 2005. Link between aerosol hygroscopic growth and droplet activation observed for hill-capped clouds at connected flow conditions during FEBUKO. *Atmos. Environ*. 39: 4247–4256.

Nenes A., Ghan S., Abdul-Razzak H., Chuang Y. & Seinfeld J.H. 2001. Kinetic limitations on cloud droplet formation and impact on cloud albedo. *Tellus* 53B: 133–149.

Rosenfeld D., Lohmann U., Raga G.B., O'Dowd C.D., Kulmala M., Fuzzi S., Reissell A. & Andreae M.A. 2008. Flood or drought: how do aerosols affect precipitation? *Science* 321: 1309–1313.

Saarikoski S., Mäkelä T., Hillamo R., Aalto P., Kerminen V.-M. & Kulmala M. 2005. Physico-chemical characterization and mass closure of size-segregated atmospheric aerosols in Hyytiälä, Finland. *Boreal Env. Res*. 10: 385–400.

Snider J.R., Guibert S., Brenguier J.-L. & Putaud J.-P. 2003. Aerosol activation in marine stratocumulus clouds: 2. Köhler and parcel theory closure studies. *J. Geophys. Res*. 108(D15), 8629, doi:10.1029/2002JD002692.

Wang J., Daum P.H., Kleinman L.I., Lee Y.-N., Schwartz S.E., Springston S.R., Jonsson H., Covert D. & Elleman R. 2007. Observation of ambient aerosol particle growth due to in-cloud processes within boundary layers. *J. Geophys. Res*. 112, D14207, doi:10.1029/2006JD007989.